# Testing and Maturing a Mass Translating Mechanism for a Deep Space CubeSat

Alex Few[1], Tiffany Lockett[2], Richard Wilson[3], David Boling[4], and Erik Loper[5]

## Abstract

**Near Earth Asteroid (NEA) Scout is a deep space satellite set to launch aboard NASA's Exploration Mission 1. The spacecraft fits within a CubeSat standard 6U (about 300 x 200 x 100 mm) and is designed to travel 1 AU over a 2.5 year mission to observe NEA VG 1991. The spacecraft will use an 86 $m^2$ solar sail to maneuver from lunar orbit to the NEA. One of the critical mechanisms aboard NEA Scout, the Active Mass Translator (AMT), has gone through rigorous design and test cycles since its conception in July of 2015. The AMT is a two-axis translation table required to balance the spacecraft's center of mass (CM) and solar sail center of pressure (CP) while also trimming disturbance torque created by off-nominal sail conditions. The AMT has very limited mass and volume requirements, but is still required to deliver a large translation range—about 160 x 68 mm—at sub mm accuracy and precision. The system is constrained to operate in complete exposure to space with limited power and data budgets for mechanical and thermal needs. The NEA Scout team developed and carried out a rigorous test suite for the prototype and engineering development unit (EDU). These tests uncovered numerous design failures and led to many failure investigations and iteration cycles. A paper was previously presented at the 43rd Aerospace Mechanisms Symposia entitled, "Development of a High Performance, Low Profile Translation Table with Wire Feedthrough for a Deep Space CubeSat". This paper will make note of specific lessons learned: manufacturing philosophy, testing ideologies for high-risk missions, thermal mitigation design for small, motor-driven mechanisms.**

## Introduction

The Near Earth Asteroid (NEA) Scout flight mission discovered the need for an active mechanism for controlling the location of center of pressure in relation to the center of mass during the early design phase of the mission, post preliminary design review. The Active Mass Translator (AMT) design passed through Critical Design Review in July 2016 with minimum breadboard and benchtop testing. The engineering team planned and prepared test procedures, facilities and a rigorous test schedule to meet the approaching flight hardware delivery date at the time. Due to resource constraints, the AMT design and development was handled by the same team producing the solar sail subsystem (Figure 1).

[1] George C. Marshall Space Flight Center, 256-544-6490, alexander.c.few@nasa.gov
[2] George C. Marshall Space Flight Center, 256-961-1304, tiffany.lockett@nasa.gov
[3] Jacobs Technologies, George C. Marshall Space Flight Center, 256-544-4079, richard.d.wilson@nasa.gov
[4] Jacobs Technologies, George C. Marshall Space Flight Center, 256-544-8648, david.a.boling@nasa.gov
[5] George C. Marshall Space Flight Center, 256-544-2668, erik.r.loper@nasa.gov

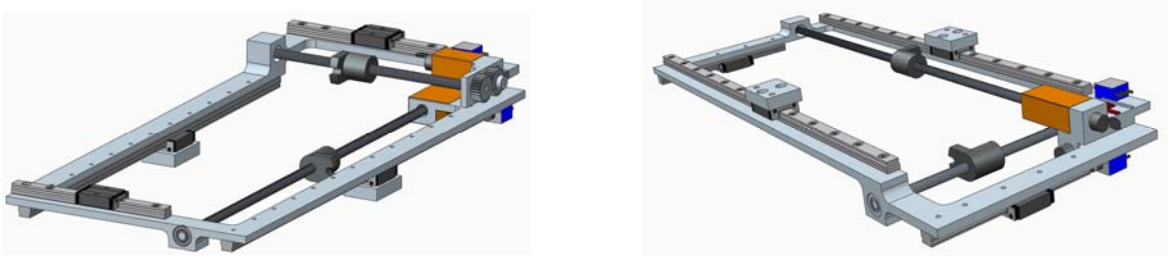

**Figure 1. Two views of the AMT at 2016 design review**

The late addition to the flight mission introduced a schedule, cost, and volume constraint that maintained minimal margins for design development. The test approach for this high risk project was to perform as needed development tests with prototype units and environmental tests on a high fidelity design unit. The team utilized 3D printed ABS plastic prototypes, commercial parts and motors, and ambient environments to perform first order functional tests.

For the prototype units, the project accepted the risk of an outside vendor using CAD models to produce the mechanical parts. The cost and schedule approach was advantageous due to the low cost for each piece part and the quick turnaround for product delivery. The out of house manufacturing shop imported CAD models and produced hardware without needing a formal drawing. Navigating around the formal drawing release process reduced schedule by 6 weeks.

To reduce risk for the flight unit, the team adhered to the MSFC flight hardware approved vendor list which did not include the manufacturing shop that produced the high fidelity engineering units. This decision cost the project time with reintroducing the hardware to a new manufacturer. The flight hardware manufacturing company still operated with released drawings and configuration control. The drawings up to that point in the project were only issued drawings, requiring little oversight and signatures. The team had to build flight quality release drawings and adhere to the quality control process.

Class D high risk missions have the ability to tailor center level mandates for development flight hardware build and manufacturing. The institutional understanding of that tailored approach was a technical and programmatic challenge. A major lesson learned was to clearly communicate and repeat constantly the project approach and risk posture for accepting lean manufacturing and acceptance processes. The knowledge lost between the development hardware manufacturer and the flight hardware manufacturer was not negligible. The team learned that using the same manufacturer for development and flight in the future would greatly reduce the quality assurance concerns upon flight hardware acceptance.

## Repairing a Poor Thermal Design

After the engineering development unit (EDU) hardware was manufactured, accepted, and assembled on center, the benchtop and environmental testing was able to commence. The team planned full functional tests, small lab vibration tests, thermal bake out, and thermal vacuum test. The thermal vacuum test followed the same temperature profile as the solar sail subsystem and utilized MSFC environment test chambers. The on-site location was beneficial for off-nominal hour support.

The purpose of the thermal vacuum testing was to demonstrate the full functionality of the system in estimated limits of the cold and hot environments to be experienced on orbit. The engineering unit went through a thermal bake out for contamination control reasons at 80°C. The engineering unit was expected to see cold temperatures at -70°C and hot temperatures at 70°C. The unit would cycle through the hot and cold temperatures four times in vacuum with functional tests completed before test, during each cold and hot cycle, and after the test was completed.

The first thermal vacuum test had a successful functional test completed before the chamber door was closed. The ambient temperature was 23°C. Once the door was closed and before vacuum pumpdown, the

AMT performed a limited functional test to ensure connection to the hardware was maintained. The test was completed successfully. After vacuum pumpdown, which took approximately 8 hours to complete, the AMT was tasked to perform a limited functional test at ambient temperature with a pressure of 1.0E-5 Torr. After initial movement, the motors displayed abnormal behavior. The test was halted.

After the TVAC failure, the NEA Scout design team met and constructed a detailed fault tree to determine as many failure causes as possible. This was crucial to ensure that no stone was left unturned, nor that the personal strengths and biases led to unconscious oversight of less obvious sources. The team produced 95% answer almost immediately: The stepper motors' internal coils had overheated and shorted. This was confirmed with impedance data and a day-of conversation with the vendor.

For the next few weeks, the team unearthed 3 root causes that led to this failure. First, the control board had provided 2.25x the motors rated current. Second, the thermal design did not provide enough contact area to allow heat to escape the motors via conduction. Third, there was a clear misunderstanding of the motor's internal heat path and how residual heat could be dissipated.

The first issue, the motor overcurrent, was remedied rather quickly. The board was reprogramed to gradually accelerate the motors speed using a simple ramp. The overcurrent error had been hidden for two reasons. First, human error had the control board programmed to 2.25x nominal current. At low speeds, the ramping function is not critical and a nominal current supply can accommodate for an instantaneous change from rest to operational speed, known as a step input. The vendor noted that these motors could handle a step input up to 1000 RPMs, but our motor was set to run at about 8000 RPMs.

At lower currents, the motor was stalled because there was not enough magnetic force to accelerate the motor from rest to the desired speed. The control board current output was increased until the motor operated, and the current output was not checked against the data sheet. This was the primary error.


**Figure 2. Size comparison of 6mm stepper**

Second, the small stepper motors predominant thermodynamic process is convection. Even at 2.25x power, the motors surface temperature barely fluctuates in atmosphere giving no tactile evidence that the motors were under thermal or mechanical stress. Once the motors entered vacuum, the overcurrent compounded by a poor thermal path led to motor failure in just seconds. Figure 2 shows the actual size of the motors and Figure 3 shows results from bench top tests comparing surface temperature rise versus time for multiple current inputs.

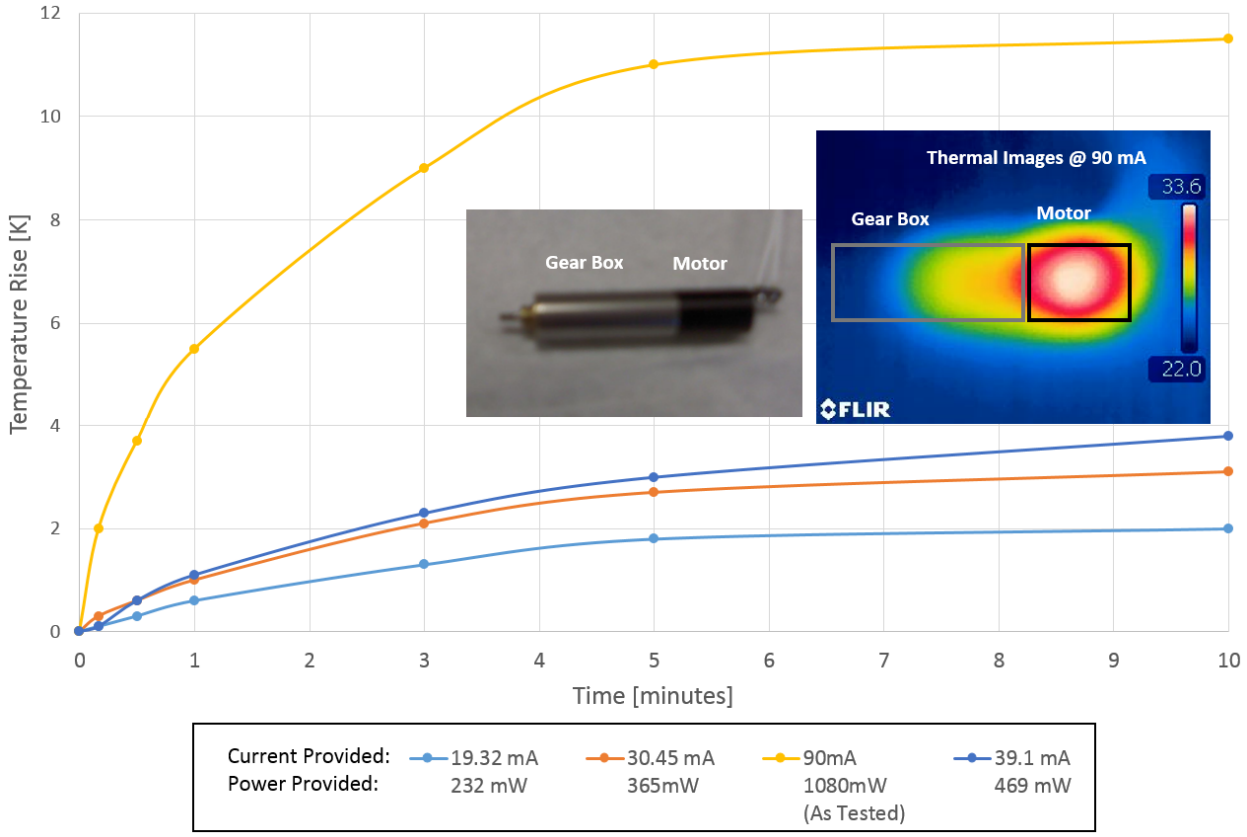


**Figure 3. 6mm stepper motor temperature rise vs. time with varying current inputs to determine sensitivity to conduction.**

The motors did not have suitable mechanical joints to the structure to allow for effective thermal conduction. Early in the design phase, the motor vendor provided mechanical fastening information. Their suggestion—to clamp the motors on the gearbox end near the output shaft—was typical for most applications, but we soon learned that our vacuum environment required a very different design (Figure 4).

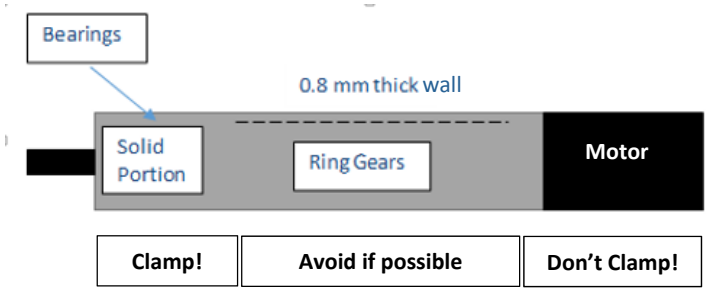


**Figure 4. Simple motor diagram showing where clamps should be applied (near left-most areas, away from the motor).**

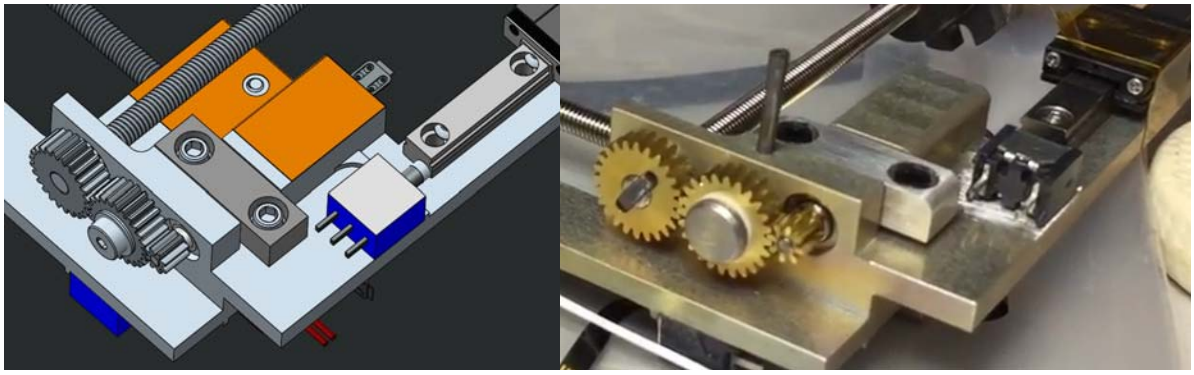

**Figure 5. Application of clamping suggestion, CAD on left, EDU on right.**

The motors had been clamped near the end of the gearbox, a location opposite of the motor coils (Figure 5). Due to the construction of the motor, the gearbox and clamps were almost completely thermally isolated from the heat source due to little contact areas between internal ball bearings, planetary gears, and a magnetically powered rotor. Therefore, the design did not allow a conduction path between the coils and the AMT structure.

The FDM0620 motors, not including the gearbox, are the same size as a mechanical pencil eraser and weigh just 1 gram. With negligible surface area and thermal mass, the 0.5 W of power destroyed the motors in seconds. FLIR images, as seen in Figure 3, show the case temperatures elevating just a few degrees above ambient in atmosphere, even without any significant external conductive path. More accurate thermal models estimated temperature deltas in the 200°C range for vacuum if the conductive path went unchanged.

A new clamp design and thermal interface material was used to mitigate the issue. The new clamps covered almost all of the motor's cylindrical surface and a thin layer of conductive material added between the two clamp halves and the motor and gearbox casings (Figure 6). Three interface materials such as conductive greases, epoxies, and thermal springs were traded. Figure 7 shows the updated thermal analysis results without thermal interface materials, then compares the three interface material options. The three bars for each data set show the steady state coil temperature at 70°C, 20°C and -70° C.

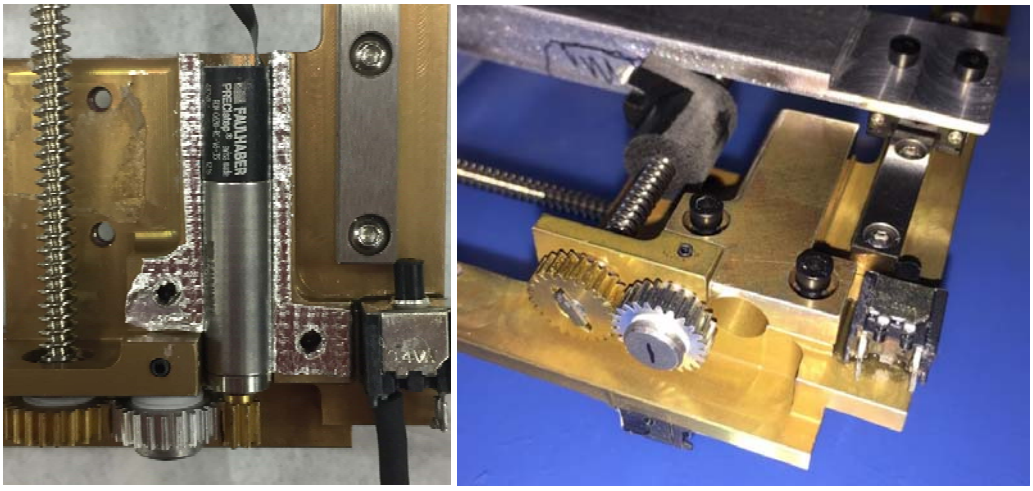

**Figure 6. New clamp design: a motor test fit (L) and a motor-less clamp fit up (R).**

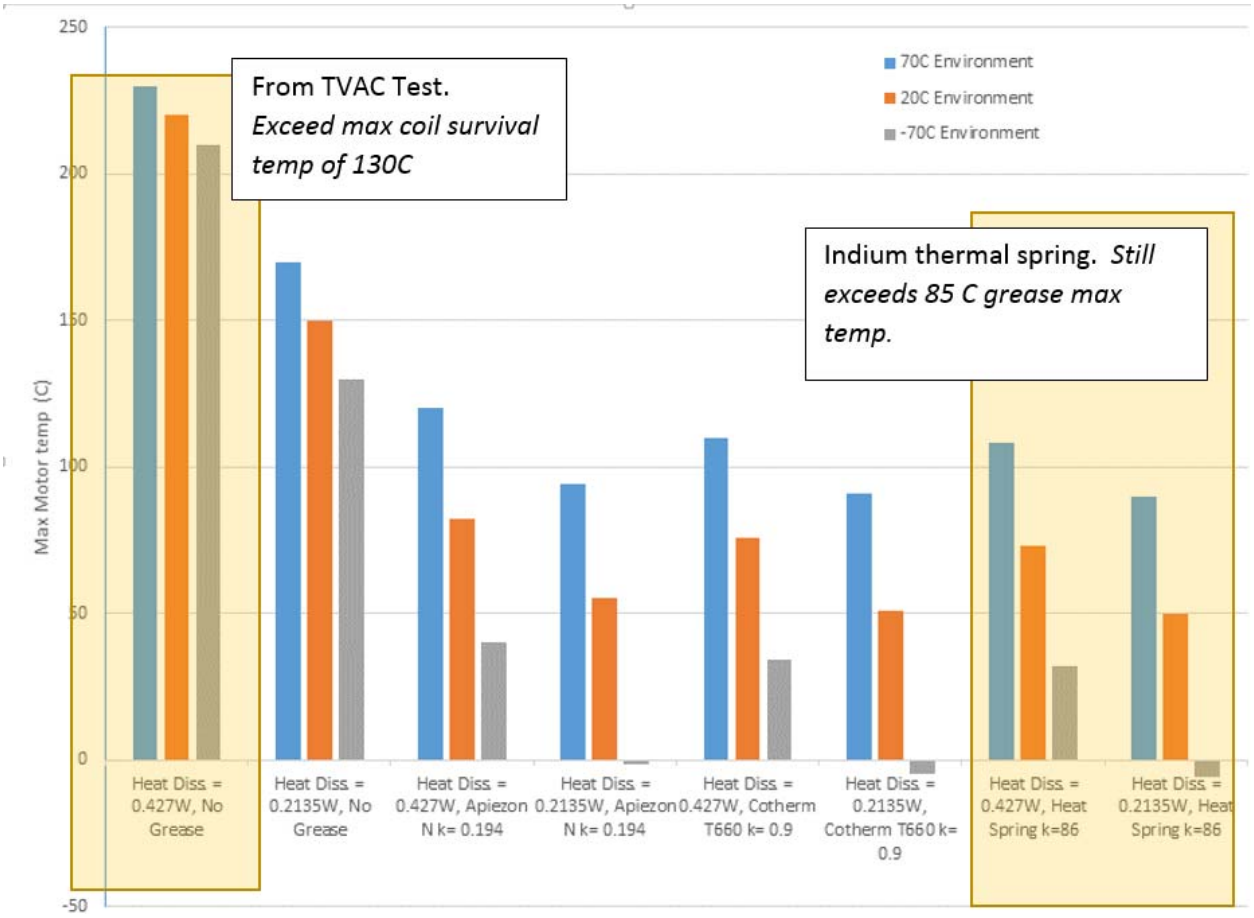


**Figure 7. Thermal analysis data after updating internal conductive paths. Three conductive material were traded at varying temperatures and heat dissipation levels: Apiezon thermal grease, Cotherm T660, and Indium heat spring.**

The 8 columns are divided into 4 pairs. Each pair describes the maximum temperature for each clamp interface material option. The first column is for when both AMT motors are powered, producing 427 mW of residual heat, and the second column describes one motor under power, producing 213 mW of residual hear.

Requirements to avoid offgassing, have a very high thermal conductivity, and simple disassembly directed the team towards the indium thermal spring. This material has high thermal conductive properties, is compressible (allowing for machining tolerances and clamping applications), and is common in space flight electronics. After taking a few weeks to redesign the AMT chassis to include the larger clamps and indium interface material, the team then set to properly understand the motor's internal conductive path (Figure 8).

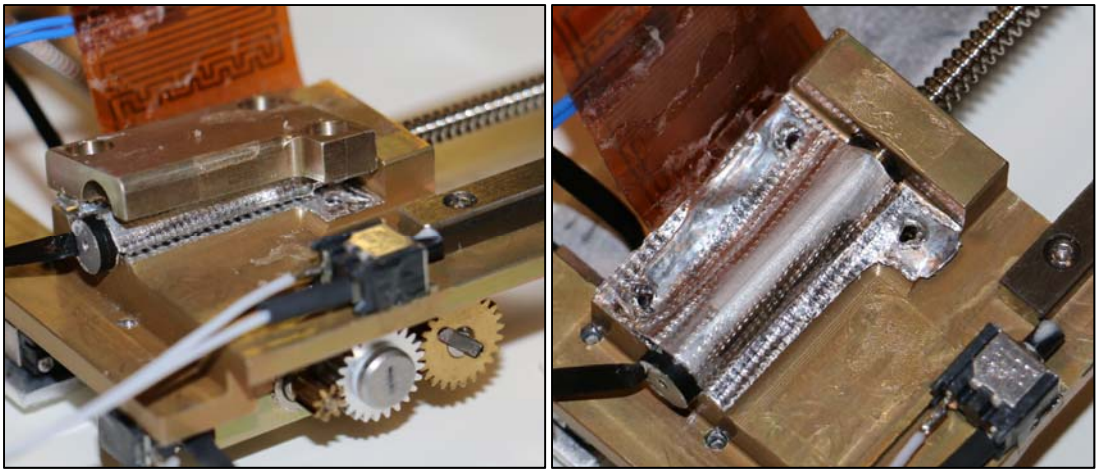

**Figure 8. New clamp design showing compressed indium. Notice the textures. This perforated surface is characteristic of the uncompressed material. The indium sheet will flatten when compressed.**

The third issue uncovered during the failure investigation was the team's lack of knowledge of the motors internal design. Though it is common for vendors not to present *all* design data for a customer, we asked, and asked often. The vendor was responsive, uncommonly understanding and provided all data that was available.

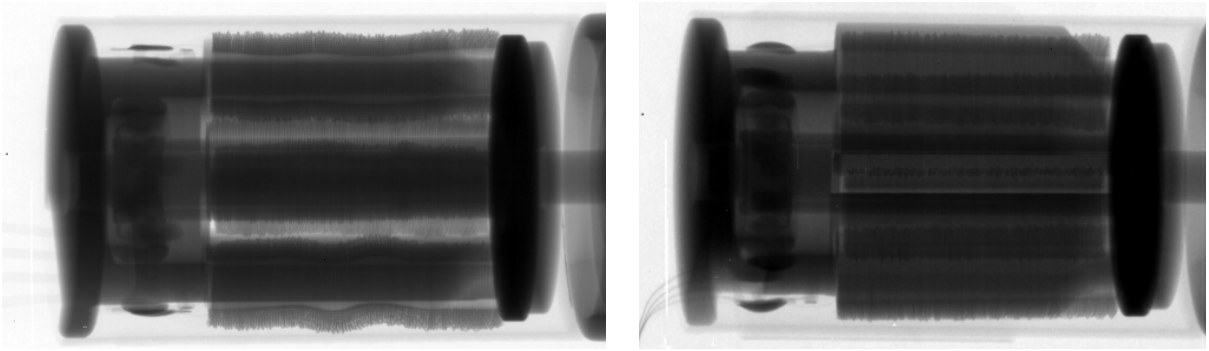

**Figure 9. X-ray of failed motor (left) and new motor (right). Note the irregularities in the failed motor most likely created from temperature spikes.**

In addition to consulting the vendor for internal design information, the team conducted non-destructive evaluation using X-ray (Figure 9). The team took X-rays of 4 failed vacuum test motors and 10 untested motors. The team compared the internal images to datasheets to determine that even our understanding of the heat path even after weeks of collaboration with the vendor was still inaccurate. It became clear that the motors were not as readily suitable for vacuum as expected. The conductive paths were miniscule, even compared to the motors small stature. Heat was conducting through multiple small junctions before ever reaching the motor casing. This was proof that the coils were reaching incredible temperatures before the motor surface measured any change.

Thermal analyses were updated with the new conductive path information and produced results more consistent with the data from the first test. The analysis referenced in figure 7 showed that coil temperatures rise about 100°C above their maximum survival temperature to nearly 230°C. During that time, the gearbox was seeing minimal thermal changes. The TVAC test thermocouple data confirmed that this updated analysis was more accurate. The figure below compares the thermal paths required under the old and new clamp designs (Figure 10).

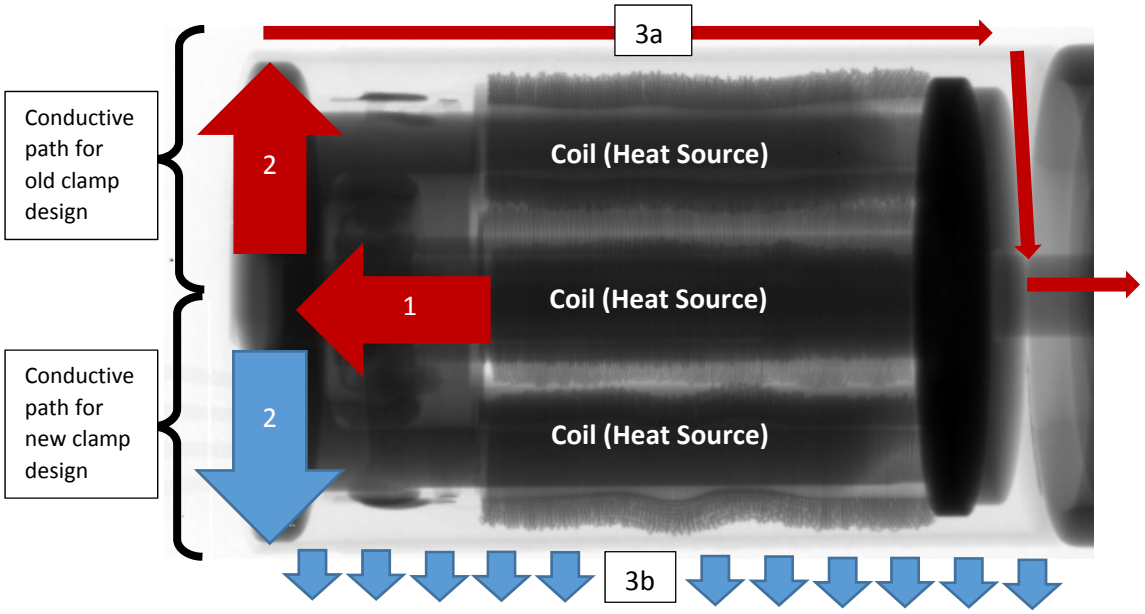


| | |
|---|---|
| 1: | Coil residual heat conducts through stator into rear cover. |
| 2a: | Heat conducts to outer cover through sub-mm thick rear cover interface. |
| 3a: | Heat conducts though motor cover, into threaded interface at rear of gearbox |
| 3b: | Heat conducts out of motor cover into indium interface material |

**Figure 10. Thermal Path Explained: old clamp design vs. new clamp design.**

Further complicating the issue, we had been relying on thermocouple data coming from the motor case and clamp to determine motor health. The thermal disconnect between the coils, case, and clamp voided our previous data and left us unsure how we could properly monitor motor health during a TVAC test. Thermocouple data from the motor surfaces had limited value due to poor internal conduction and the motors size did not allow internal monitoring with any test equipment. The team had no way to determine the motor's health with any available test equipment and any data received was of little value to determining the motor's coil status.

Eventually, the team realized that the motor coils were essentially a pair of resistance temperature detectors (RTDs). Any temperature change in the copper coils would correlate to a measurable impedance change and we could use this principal to determine the motor's internal temperature. The principal equation is shown below:

$$R(T) = R_0(1 + \alpha(T_c - T_0)) \quad [1]$$

Which could be applied as follows:

$R(T) = coil\ impedance\ at\ test\ environment\ temperature$
$R_0 = coil\ impedance\ at\ room\ temperature\ (120\ \Omega)$
$\alpha = coefficient\ of\ thermal\ resistance\ for\ coil\ material\ (copper = 0.0039\ {}^{\Omega}/_{\circ C})$
$T_c = coil\ temperature\ at\ test\ environment\ temperature$
$T_0 = room\ temperature\ (20\ ^{\circ}C)$

Giving the impedance-driven relationship for our experiment:

$$T_c = T_0 + \frac{\frac{R(T)}{R_0} - 1}{\alpha} = 20 + \frac{\frac{R(T)}{120} - 1}{0.0039} \quad [2]$$

This simple relationship between the coil temperature and impedance altered our test ideologies. The team now had a method of instantaneously measuring the coils temperatures at vacuum and could relate a max coil temperature to an ambient environment to determine operational ranges. The team conducted a new TVAC test aimed to determine the operation range for these motors in their new thermally-optimized design. The test ran each motor in vacuum for 15 minutes to achieve steady state. The motors were then powered off and the coil impedances were measure immediately after shutdown. The data was recorded and used to determine a max coil temperature at a given chamber ambient temperature.

The data was coarse, and even a few seconds of delay between shutdown and measurement would result in 10°C temperature drops (the coils are less than 1 gram each). The chamber was then heated up from -50°C by 5°C increments until the coils reached their maximum survival temperature. The data showed a striking trend, providing the test data needed to determine the thermal design was sufficient and the AMT operation range was well-founded. The chart below shows the temperature data collected from the AMT X and Y-axis motors, each having two coils, notated as "A" and "B" (Figure 11). The four data sets were plotted against the chamber temperature and the tests concluded when the hottest coil measurement crossed the maximum coil survival temperature of 130°C.

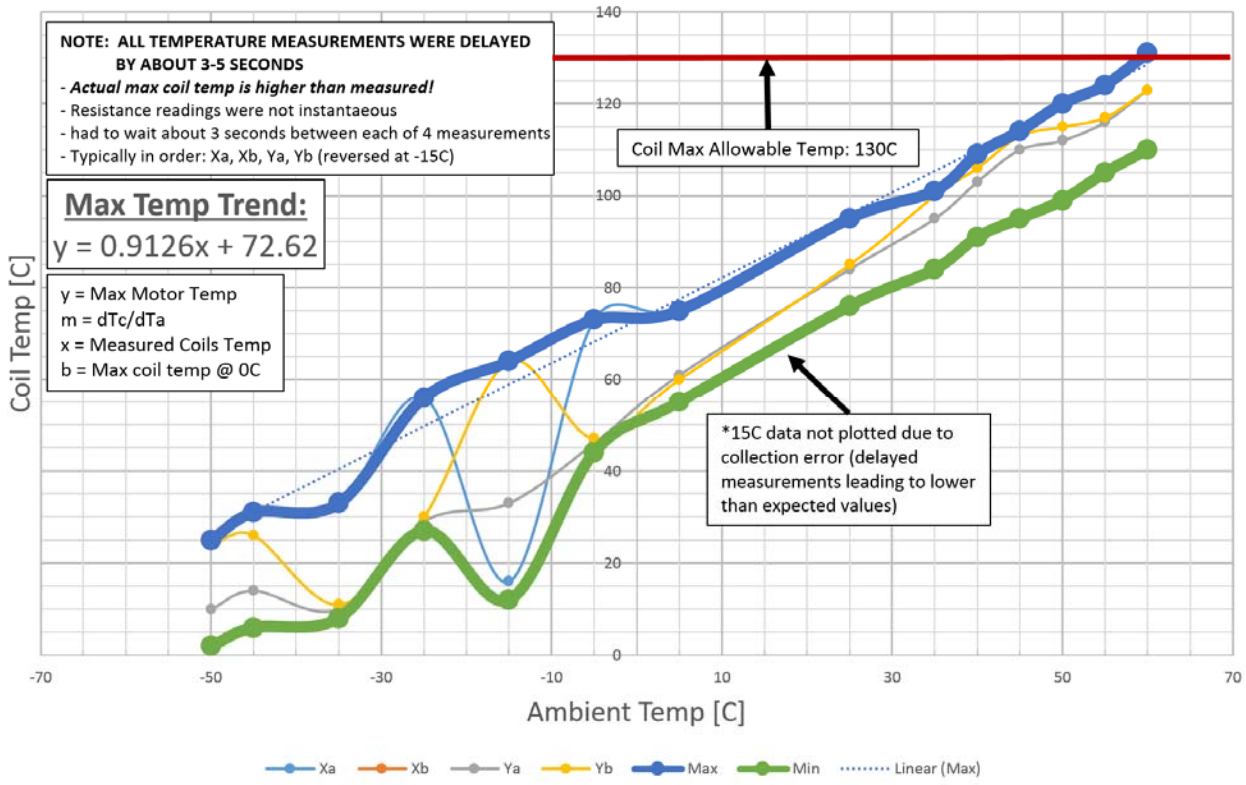


**Figure 11. AMT motor coil temperature vs. vacuum chamber ambient temperature. Data collected using coil impedance measurements and temperatures calculated using equation 1.**

## Conclusion

After a lengthy design trade, a 6 mm stepper motor from Faulhaber (FDM0620) was selected for the EDU design. (If interested in more details from the design trade, please reference “Development of a High Performance, Low Profile Translation Table with Wire Feedthrough for a Deep Space CubeSat” from the 43rd Aerospace Mechanisms Symposium). These motors were the smallest available anywhere on the FY2015 market and were manufactured from a reputable vendor with flight heritage. Motors from this two phase, PRECIstep ® family had flown and were planning to fly on multiple NASA missions, including another 6U CubeSat manifested on SLS EM-1. Knowing this, it was assumed that the motors would operate in a vacuum environment once integrated into the AMT.

After a year of failure investigations and redesigns, the motors performed in vacuum within the operational temperature ranges determined by our thermal design during thermal vacuum tests. The lessons learned have been captured at the project level through engineering review board documentation. There is a miniscule market for flight qualified stepper motors in mNm torque magnitudes. If small motors like these are required to meet mass, power, and volume budgets in vacuum, a thorough investigation and test plan should be implemented to validate their application.

The project could have saved considerable time and cost by budgeting a few thousand dollars to purchase a small vacuum chamber and test as often as needed, rather than invest months of labor and facility costs to purchase multiple high fidelity tests. Small vacuum chambers with the data output required to thoroughly test the motors in the correct thermal and vacuum environment are difficult to find on center without a cost and schedule burden.

Development of the AMT flight unit was an excellent opportunity for the young NEA Scout team to learn about flight hardware testing. The team learned of the false sense of accomplishment benchtop testing can provide. Blind dependence on vendor information proved to be a cost and schedule hit that fortunately the project was able to afford at the time. Do not take any analytical data from the family-oriented documentation provided by a vendor without application confirmation or performing inspections.

In summary, the project accepted the risk of utilizing a lien approach to hardware development to help save cost and schedule. The assumptions made early in the project were with the best information gathered at the time. Without the anomalies experienced during thermal vacuum testing

The project made the right decision with reserving a large portion of the project schedule to design and development. Leveraging rapid prototyping, out of house manufacturing shops, and communicative vendors allowed the project to be successful and absorb all of the lessons learned while still delivering flight hardware. Use of the lien development process allowed to team to get familiar with the hardware and confident in the design. This gave the project confidence in accepting the flight hardware mechanism design.

## References


1. McNutt, L.; Johnson, L.; Clardy, D.; Castillo-Rogez, J.; Frick, A.; and L. Jones. “Near-Earth Asteroid Scout.” AIAA Space 2014 Conference; 4-7 Aug. 2014; San Diego, CA; United States.
2. Few, A.; “Development of a High Performance, Low Profile Translation Table with Wire Feedthrough for a Deep Space CubeSat.” 43rd Aerospace Mechanisms Symposia; 4-6 May 2016; San Jose, CA.; United States.